CRYSTAL GROWTH & DESIGN

Article

pubs.acs.org/crystal

Porous Lanthanide–Organic Frameworks: Control over Interpenetration, Gas Adsorption, and Catalyst Properties

Haiyan He,[†,§] Huiqing Ma,[‡,§] Di Sun,[‡] Liangliang Zhang,[†] Rongming Wang,[†] and Daofeng Sun*[,†,‡]

[†]College of Science, China University of Petroleum (East China), Qingdao Shandong 266580, People's Republic of China

[‡]Key Lab for Colloid and Interface Chemistry of Education Ministry, School of Chemistry and Chemical Engineering, Shandong University, Jinan 250100, People's Republic of China

Supporting Information

ABSTRACT: Two isomorphous lanthanide–organic frameworks, $Ln(BDC)_{1.5}(DMF)(H_2O)$ (Ln = Er (**1**), Tm (**2**)) have been synthesized based on 1,4-benzenedicarboxylic acid (H_2BDC). Because of the 2-fold interpenetration, the pores are partly blocked and there are no significant gas adsorptions for these two interpenetrating nets. Through control over interpenetration by applying an organic ligand with hindrance groups or replacing coordinated solvent molecules with a chelating ligand, three non-interpenetrating lanthanide–organic frameworks, $Er_2(BDC)_3(phen)_2{\cdot}3H_2O$ (**3**), $Tm(TBDC)_{1.5}(DMF)(H_2O){\cdot}2H_2O$ (**4**), $Er_2(TBDC)_3(phen)_2{\cdot}4DMF{\cdot}2H_2O$ (**5**), possessing the same topology with **1** and **2**, have been synthesized and characterized. Further changing reaction conditions, three other porous lanthanide–organic frameworks with different structures with **1**–**5**, $Tm(BDC)_{1.5}(H_2O){\cdot}0.5DMF{\cdot}C_2H_5OH{\cdot}2H_2O$ (**6**), $Tm_4(BDC)_6(H_2O)_2(DMF)(C_2H_5OH){\cdot}2DMF{\cdot}2H_2O$ (**7**), and $Sm(TBDC)_{1.5}(phen)(H_2O){\cdot}DMF{\cdot}H_2O$ (**8**), have been constructed. Gas sorption measurements for **5**, **6**, **7**, and **8** have been carried out and revealed that these materials possess permanent porosity. The catalytic property for complex **6** has also been studied.

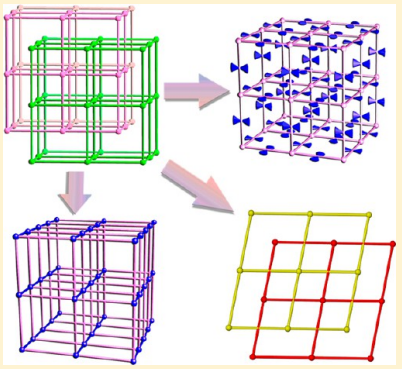

1. INTRODUCTION

The construction of porous metal–organic frameworks (MOFs) has received much interest because of their fascinating topologies and intriguing potential in applications such as catalysis science, separation and gas storage, etc.[1−5] Although many MOFs with large channels have been synthesized and reported, the removal of the coordination solvent molecules from the crystalline framework was frequently accompanied by the collapse of the structure.[6] In particular, lanthanide ions have high affinity for oxygen donor atoms and possess high coordination numbers when they are coordinated in conjunction with bridging or chelating ligands.[7] Because of the steric hindrance between the organic ligands, it is challenging that all the coordination sites of the lanthanide ion are occupied by the organic ligands. In the reported lanthanide–organic frameworks, most of the remaining coordination sites of the lanthanide ions are occupied by coordinated solvates such as H_2O, DMF, etc.[8,9] The coordinated small solvates are easy to be removed from the lanthanide ions, which results in the formation of unstable low-coordinated lanthanide ions and further causes the collapse of the whole framework. The more coordination sites of the lanthanide ions are occupied by the solvates, the more likely the porous frameworks thermally collapse. Construction of open lanthanide-organic framework with permanent porosity is still a great challenge to chemists.[10]

As is known, the appropriate size of pores shows great advantages in gas storage or adsorption properties of crystalline structures. Obviously, the effective strategy to increase the porosity of an MOF might be to extend the size of the ligand sustaining the framework.[11] However, because of large windows or channels in the structure, it is not surprising that interpenetration or an interweaving framework always appears to stabilize the structure.[12,13] On the other hand, interpenetration might limit the size of the pores in crystal frameworks, which influences the gas sorption property dramatically. Considering the two aspects, two strategies can be applied: one is to apply organic ligand containing large hindrance groups to prevent the formation of interpenetration, and these hindrance groups can reduce the size of the channels while inducing reasonable pore canals; the other one is to use *in situ* generated rod-shaped secondary building units (SBUs) reported by Yaghi and co-workers, the rigidity of the rod-shaped SBUs effectively avoids interpenetration, thus improving the porosity of the frameworks.[14] The first strategy mentioned above has been studied lately;[12a,15] however, most of these studies were based on control over interpenetration by using organic building blocks but ignoring the influences of gas sorption capability. Meanwhile, little attention has been paid in applying two-dimensional sheets or layered structures to develop the potential gas adsorptions considering its compact stacking mode and high thermal stability.[16] In this study, we

Received: April 10, 2013
Revised: April 18, 2013
Published: May 15, 2013

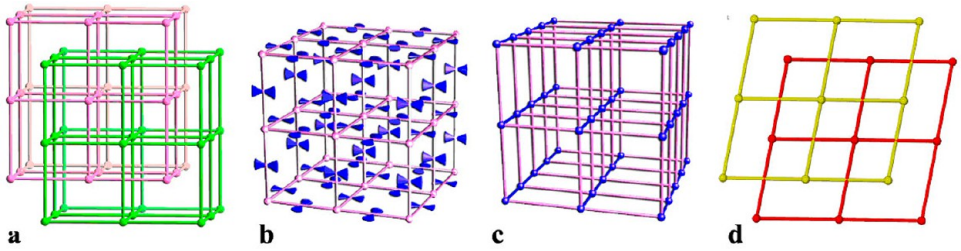

Figure 1. Schematic representation of the interpenetrating net without channels (a), the porous non-interpenetrating nets constructed by organic ligand with a large steric-hindrance group (b), inorganic rod-shaped SBUs (c), and two-dimensional compact stacking layers (d).

focus on the construction of porous lanthanide-organic frameworks and their gas adsorption (figure 1).

As a result, four types of lanthanide−organic frameworks are presented: type I: $Ln(BDC)_{1.5}(DMF)(H_2O)$ (Ln = Er (**1**), Tm (**2**), H_2BDC = 1,4-benzenedicarboxylic acid, DMF = *N*,*N*-dimethylformamide), with 2-fold interpenetrating three-dimensional frameworks;[12a] type II: $Er_2(BDC)_3(phen)_2·3H_2O$ (**3**), $Tm(TBDC)_{1.5}(DMF)(H_2O)·2H_2O$ (**4**), $Er_2(TBDC)_3(phen)_2$-$·4DMF·2H_2O$ (**5**) (H_2TBDC = 2,3,5,6-tetramethyl-1,4-benzenedicarboxylic acid, phen = 1,10-phenanthroline), with non-interpenetrating porous frameworks based on binuclear SBUs; type III: $Tm(BDC)_{1.5}(H_2O)·0.5DMF·C_2H_5OH·2H_2O$ (**6**) and $Tm_4(BDC)_6(H_2O)_2(DMF)(C_2H_5OH)·2DMF·2H_2O$ (**7**), with three-dimensional porous frameworks based on rod-shaped SBUs; type IV) $Sm(TBDC)_{1.5}(phen)(H_2O)·DMF·H_2O$ (**8**), with 2D layered honeycomb possessing an AAAA stacking arrangement.

2. EXPERIMENTAL SECTION

2.1. Synthesis. All chemicals and solvents used in the syntheses were of analytical grade and used without further purification. The ligand of 2,3,5,6-tetramethyl-1,4-benzenedicarboxylate (H_2TBDC) was synthesized using the literature method.[17]

*$Er_2(BDC)_3(DMF)_2(H_2O)_2$ (**1**).* A mixture of $ErCl_3·6H_2O$ (40 mg, 0.11 mmol) and H_2BDC (20 mg, 0.12 mmol) was suspended in the solution of DMF/EtOH (V/V = 2:1, 10 mL) and heated in Teflon-lined steel bomb at 110 °C for 4 days. The pink block crystals were collected, washed with water, and dried in the air. Yield: 64% (based on H_2BDC). Elemental analysis calcd (%) for 1: C 35.71, H 3.00, N 2.78; found: C 35.13, H 3.16, N 3.24.

*$Tm_2(BDC)_3(DMF)_2(H_2O)_2$ (**2**).* The procedure to synthesize complex **2** was similar to that of complex **1**, except that the $ErCl_3·6H_2O$ was replaced by $Tm(NO_3)_3·3H_2O$. Yield: 51% (based on H_2BDC). Elemental analysis calcd (%) for **2**: C 35.59, H 2.97, N 2.77; found: C 35.88, H 3.20, N 3.05.

*$Er_2(BDC)_3(phen)_2·3H_2O$ (**3**).* A mixture of $ErCl_3·6H_2O$ (40 mg, 0.11 mmol), H_2BDC (20 mg, 0.12 mmol), 2,2-bpy (10 mg, 0.06 mmol), and phen (10 mg, 0.06 mmol) was suspended in mixed solution of DMF/EtOH/H_2O (V/V = 5:2:1, 15 mL) and heated in an uncovered tube at 50 °C for 3 days. The formed pink needlelike crystals were collected, washed with ethanol, and dried in the air. Yield: 63% (based on H_2BDC). Elemental analysis calcd (%) for **3**: C 46.44, H 2.76, N 4.51; found: C 45.98, H 2.89, N 4.35.

*$Tm_2(TBDC)_3(DMF)_2(H_2O)_2·4H_2O$ (**4**).* A mixture of $Tm(NO_3)_3·3H_2O$ (40 mg, 0.10 mmol) and H_2TBDC (20 mg, 0.09 mmol) was suspended in mixed solution of DMF/EtOH/H_2O (V/V = 5:2:1, 15 mL) and heated in an uncovered tube at 30 °C for two weeks. The colorless prism crystals were collected, washed with ethanol, and dried in the air. Yield: 53% (based on H_2TBDC). Elemental analysis calcd (%) for **4**: C 40.27, H 4.99, N 2.24; found: C 39.98, H 4.82, N 2.31.

*$Er_2(TBDC)_3(phen)_2·4DMF·2H_2O$ (**5**).* A mixture of $ErCl_3·6H_2O$ (40 mg, 0.11 mmol), H_2TBDC (20 mg, 0.09 mmol), and phen (10 mg, 0.06 mmol) was suspended in mixed solution of DMF/EtOH/H_2O (V/V = 5:2:1, 15 mL) and heated in an uncovered tube at 50 °C for 3 days. The light pink needlelike crystals were collected, washed with ethanol, and dried in the air. Yield: 51% (based on H_2TBDC). Elemental analysis calcd (%) for **5**: C 51.35, H 5.03, N 6.65; found: C 50.35, H 4.64, N 6.52.

*$Tm(BDC)_{1.5}(H_2O)·0.5DMF·C_2H_5OH·2H_2O$ (**6**).* A mixture of $Tm(NO_3)_3·3H_2O$ (40 mg, 0.086 mmol), H_2BDC (20 mg, 0.12 mmol), and 2,2-bpy (10 mg, 0.06 mmol) was suspended in mixed solution of DMF/EtOH/H_2O (V/V = 5:2:1, 15 mL) and heated in an uncovered tube at 50 °C for 7 days. The colorless plate crystals were collected, washed with ethanol, and dried in the air. Yield: 53% (based on H_2BDC). Elemental analysis calcd (%) for **6**: C 33.74, H 3.93, N 1.27; found: C 34.12, H 4.23, N 1.35%.

*$Tm_4(BDC)_6(H_2O)_2(DMF)$ $(C_2H_5OH)·2DMF·2H_2O$ (**7**).* A mixture of $Tm(NO_3)_3·3H_2O$ (40 mg, 0.086 mmol), H_2BDC (20 mg, 0.12 mmol), and phen (10 mg, 0.06 mmol) was suspended in mixed solution of DMF/EtOH/H_2O (V/V = 1:1:1, 15 mL) and heated in an uncovered tube at room temperature for 6 weeks. The colorless plate crystals were collected, washed with ethanol, and dried in the air. Yield: 53% (based on H_2BDC). Elemental analysis calcd (%) for **7**: C 35.47, H 2.98, N 2.10; found: C 35.12, H 2.83, N 2.23%.

*$Sm(TBDC)_{1.5}(phen)(H_2O)·DMF·H_2O$ (**8**).* The procedure to synthesize complex **8** was similar to that of complex **5**, except that the $ErCl_3·6H_2O$ was replaced by $Sm(NO_3)_3·3H_2O$. Yield: 51% (based on H_2TBDC). Elemental analysis calcd (%) for **8**: C 51.47, H 4.84, N 5.46; found: C 50.48, H 4.27, N 5.44%.

2.2. Physical Measurements. ^1H NMR spectra was measured with a Bruker AVANCE-300 NMR spectrometer. Elemental analyses (C, H, N) were achieved with a PerkinElmer 240 elemental analyzer. The thermogravimetric analysis (TGA) was carried out from room temperature to 800 °C in a static N_2 with a heating rate of 10 °C/min (Figures S1−S3, Supporting Information). The low-pressure N_2 and H_2 sorption isotherm measurements were performed with an ASAP 2020M accelerated surface area and porosimetry analyzer.

2.3. Crystal Structure Determination. The intensity data of **1**−**8** were collected at 173 K with a Bruker Apex II area detector diffractometer (Mo Kα, λ = 0.71073 Å). Absorption corrections was achieved by using the multiscan method. Data were integrated and corrected for Lorentz, polarization, and absorption effects. Space group determinations were made based on systematic absences, E statistics, and successful refinement of the structure. Structures were solved by direct method and refined by full-matrix least-squares on F^2 using *SHELXTL*.[18] Non-hydrogen atoms were refined with anisotropic displacement parameters during the final cycles. Organic hydrogen atoms were placed in calculated positions with isotropic displacement parameters set to 1.2 or 1.5 × U_{eq} of the attached atom.

3. RESULTS AND DISCUSSION

3.1. Structure Descriptions. *$Ln(BDC)_{1.5}(DMF)(H_2O)$ (Ln = Er (**1**), Tm (**2**)).* X-ray single crystal diffraction reveals that complexes **1** and **2** are isomorphous. Details about the structures of **1** and **2** (denoted as structure type I) can be found in ref 12a. Several other lanthanide−organic frameworks similar to **1** and **2** have also been reported recently.[19] The central metal ion is eight-coordinated, and two such ions are

dx.doi.org/10.1021/cg400531j | Cryst. Growth Des. 2013, 13, 3154−3161

bridged by two carboxylate groups generating a binuclear SBU. The SBUs are further connected by four carboxylate groups from different BDC ligands forming a 3D framework. Two such nets interpenetrate each other to form a 2-fold interpenetrating framework with *pcu* net (Figures 1 and 2).

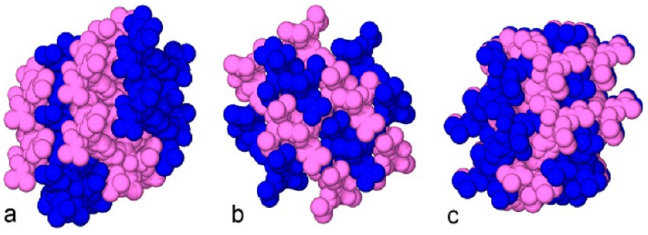

Figure 2. (a–c) The 2-fold interpenetrating nonporous frameworks of **1**, shown from the *a*, *b*, *c* axis, respectively.

Because of the interpenetration, complexes **1** and **2** are nonporous. To improve the porosity, non-interpenetrating complexes **3**–**5** possessing the same topology with **1** and **2** were synthesized by applying organic ligand with hindrance groups or replacing coordinated solvent molecules with chelating ligand.

*$Er_2(BDC)_3(phen)_2{\cdot}3H_2O$ (**3**), $Tm(TBDC)_{1.5}(DMF)(H_2O){\cdot}2H_2O$ (**4**), and $Er_2(TBDC)_3(phen)_2{\cdot}4DMF{\cdot}2H_2O$ (**5**).* The solvothermal reaction of H_2BDC/H_2TBDC, $Ln(NO_3)_3{\cdot}3H_2O$ (Ln = Er, Tm) in $DMF/EtOH/H_2O$ in the presence of phen led to the formation of prismatic crystals of **3**–**5**. Figure 3 displays the coordination environments of the central ions in these three complexes: (i) the central Er ion of **3** adopts similar coordination geometry with the Er ion in **1**, except that the coordinated DMF and water molecules in **1** are replaced by chelating phen ligand; (ii) TBDC ligand, which is a derivative organic ligand of BDC with methyl groups as hindrance, is applied in **4**; (iii) in **5**, both phen and TBDC ligands are used to replace BDC and coordinated solvent molecules. In each complex, two central ions are bridged by carboxylate groups generating the basic binuclear SBU, which is further connected by carboxylate ligands to form final framework. Thus, these three complexes (denoted as structure type II) possess the same topology with **1** (Figure 4) but have non-interpenetrating porous frameworks due to the steric hindrance of the methyl groups of TBDC and/or the coordinated phen ligands.

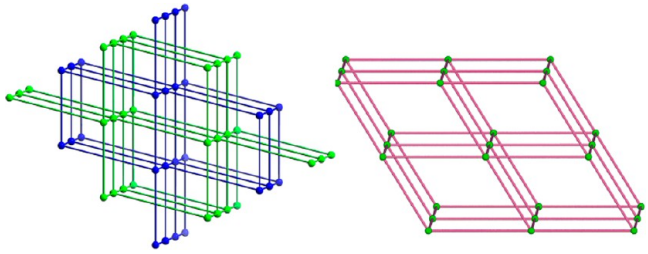

Figure 4. The same *pcu* topology with interpenetrations of **1** (left) and non-interpenetrations of **3**, **4**, and **5** (right).

*$Tm(BDC)_{1.5}(H_2O){\cdot}0.5DMF{\cdot}C_2H_5OH{\cdot}2H_2O$ (**6**) and $Tm_4(BDC)_6(H_2O)_2(DMF)_2{\cdot}2DMF{\cdot}2H_2O$ (**7**).* Compared to the discrete rigid SBU, the rod-shaped SBU can not only prevent the formation of interpenetrating nets but also significantly improve the thermal stability of the final framework. Since the SBU is *in situ* generated during the assembly procedure, it is difficult to predesign the SBU in the assembly of MOFs. However, the lanthanide ions have higher affinity for oxygen atom and possess higher coordination numbers than those of transition metal ions.[8,9] Hence, they are apt to form rod-shaped SBU during the assembly procedure. Thus, the solvothermal reaction of H_2BDC and $Tm(NO_3)_3{\cdot}3H_2O$ in different solvents resulted in the formation of complexes **6** and **7**, which crystallizes in the monoclinic space group $C2/c$ or $P\bar{1}$, respectively, and both possess slightly distinct 3D porous frameworks based on a rod-shaped SBU.

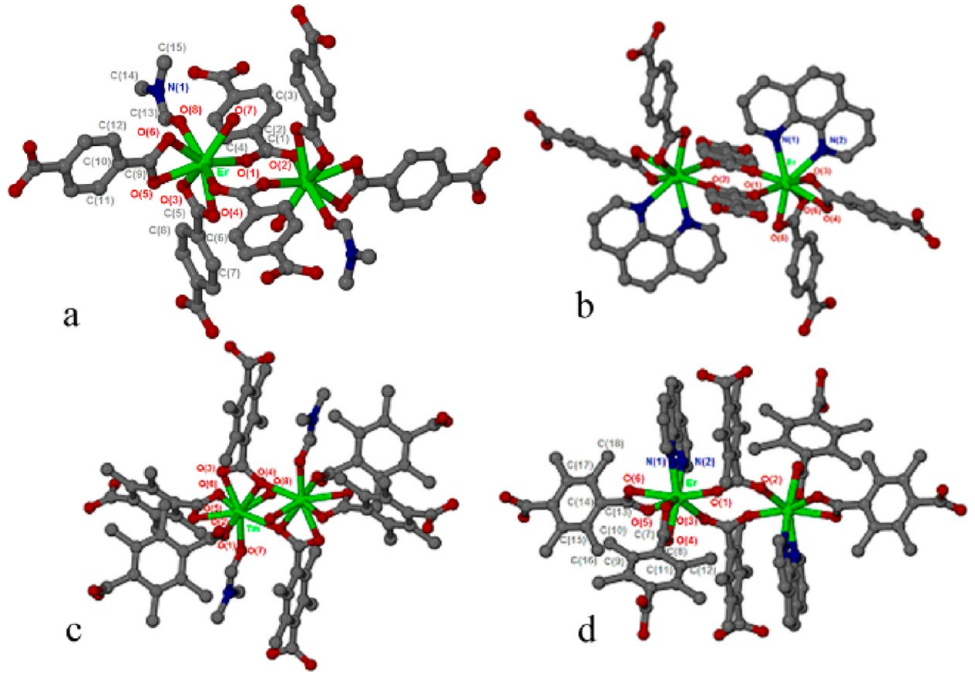

Figure 3. The comparison of coordination environments of central metal ions in **1** (a), **3** (b), **4** (c), and **5** (d).

dx.doi.org/10.1021/cg400531j | *Cryst. Growth Des.* 2013, 13, 3154–3161

The asymmetric unit of **6** consists of one thulium ion, two and a half BDC ligands, one coordinated water molecule, and one uncoordinated water molecule (Figure S1, Supporting Information). The central thulium ion is seven-coordinated by six carboxyl oxygen atoms from different BDC ligands and one coordinated water molecule, with the average Tm−O distance of 2.290 Å. Different from that in **1**, both carboxylate groups of BDC ligand adopt bidentate bridging mode to connect two thulium ions. Thus, the thulium ions are connected by carboxylate groups of BDC to generate infinite Tm−O−C rods along the [0 0 1] direction with the nearest Tm−Tm distance of 4.22 Å, which is slightly different from other studies.[20,21] The Tm−O−C rods are stacked in parallel and linked by the benzene ring of BDC forming 1D rhombic channels along the *c* axis with the dimensions of 11.6 × 11.6 Å along the edge and 16.6 × 13.2 Å along the diagonal (Figure 5),

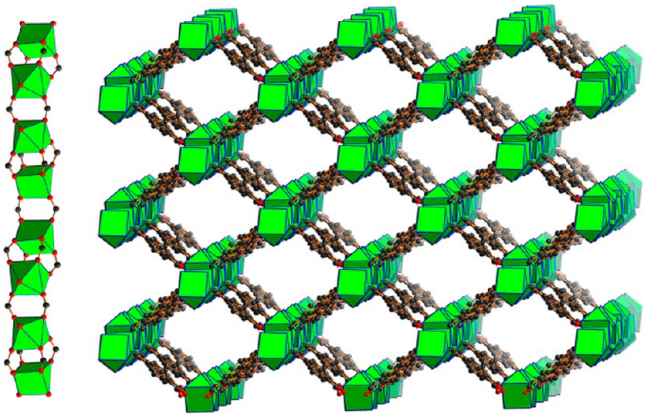

Figure 5. The inorganic rod-shaped SBU (left) showing that each carboxylate group adopts bibentate bridging mode to link two Tm ions in complex **6**, and the 3D porous framework of **6** along the *c* axis (right).

in which the uncoordinated solvates reside. As expected, due to the rigidity of the rod-shaped SBU, complex **6** is a non-interpenetrating porous framework with the solvent-accessible volume of 50.7% (calculated with PLATON[22]) after the removal of the coordinated water molecule.

Complex **7** possesses a similar inorganic rod-shape SBU like complex **6**, while its asymmetric unit consists of four thulium ions, six BDC ligands, two coordinated water molecules, two coordinated DMF molecules, and two uncoordinated DMF molecules (Figure S2). The coordination environment of central metal ions of complex **7** is similar to that of complex **6**, except the coordinated water of two adjacent thulium ions are replaced by DMF molecules. The thulium atoms are connected by carboxylate groups alternatively to form the rod-shaped SBU. Because of the coordinated DMF molecules pointing toward the channels, the size of the parallelogram channels are squeezed into two types: large channels with 10.9 × 10.8 Å along edge and 16.6 × 12.6 Å along the diagonal with free DMF molecules occupied, and a smaller one with the 10.9 × 10.7 Å along the edge and 10.8 × 17.6 Å along the diagonal with the coordinated DMF occupied (Figures 6 and S3). Complex **7** possesses less solvent occupation of crystal volume than that of **6** (42.7 vs 50.7%), calculated with PLATON.

In addition, complexes **3**−**5** decompose after 400 °C, while complexes **6** and **7** can be stable up to 560 °C. The curves of thermal-gravity analysis indicate that type II structures are less

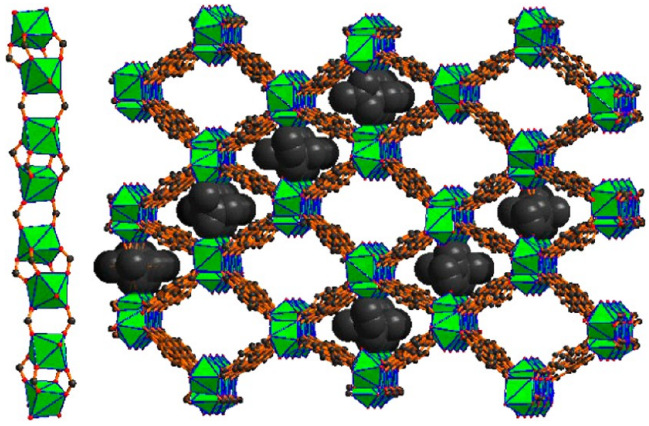

Figure 6. The inorganic rod-shaped SBU (left) showing each carboxylate group adopts bibentate bridging mode to link two Tm ions in complex **7**, and the 3D porous framework of **7** along the *b* axis (right). The coordinated DMF molecules are shown in a space-filling mode.

stable than type III structures, which further indicates the rod-shaped SBUs can effectively enhance the thermal stability of the frameworks (Figure S6).

Sm(TBDC)$_{1.5}$(phen)(H$_2$O)·DMF·H$_2$O (**8**). When $ErCl_3·6H_2O$ was replaced by $Sm(NO_3)_3·3H_2O$ in the preparation of **5**, complex **8** was obtained as colorless crystals. Single-crystal X-ray diffraction reveals that complex **8** is a layered framework with honeycomb or (6,3) net. The asymmetric unit of **8** consists of one samarium ion, one coordinated water molecule, one and a half TBDC ligands, one phen ligand, one uncoordinated DMF molecule, and one uncoordinated water molecule. The samarium ion is coordinated by six oxygen atoms from three TBDC ligands, one coordinated water molecule, and one coordinated phen molecule (Figure 7). The two carboxylate groups of TBDC ligands adopt a bidentate chelating mode to connect two adjacent metal ions. Because of the effect of the steric hindrance between carboxylate groups and methyl groups, the two carboxylate groups of TBDC ligands do not locate in a plane within the central benzene ring,

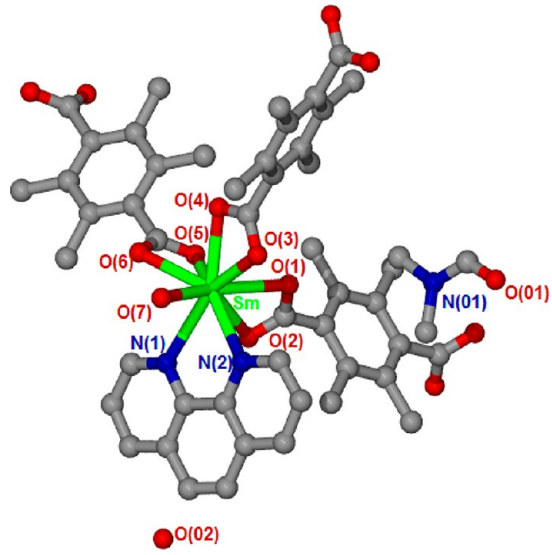

Figure 7. The coordination environment of samarium ion in complex **8**.

dx.doi.org/10.1021/cg400531j | *Cryst. Growth Des.* 2013, 13, 3154−3161

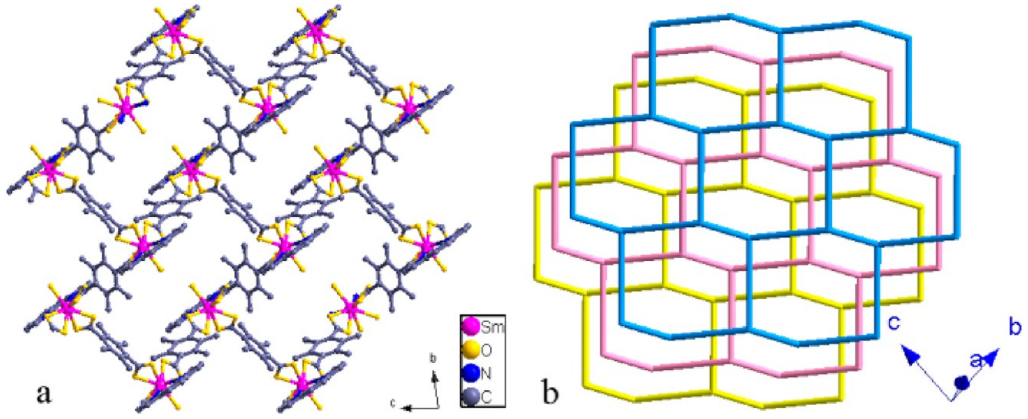

Figure 8. (a) The arrangement of single layer seen from the *a* axis in **8**; (b) the 2D honeycomb layers stacking as the AAAA form.

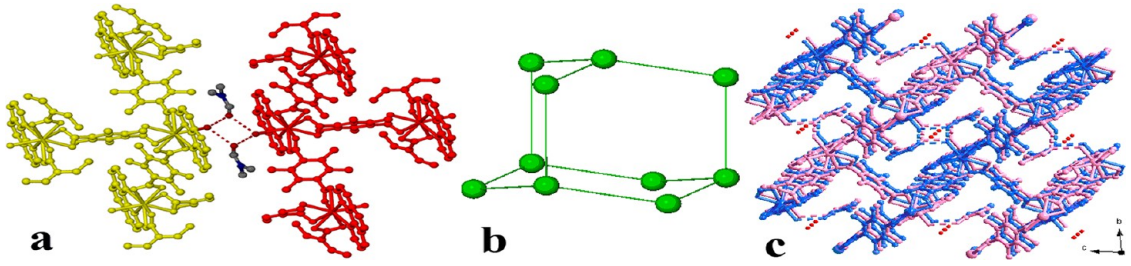

Figure 9. (a) The hydrogen bonding in dash line, (b) the simplified structure with single diamond topology of **8**, and (c) the 2-fold interpenetrating diamond structure with free water molecules in red.

and the average diheral angle between the carboxylate groups with the benzene ring is 64.9°. The different coordination geometry of central metal ions in **5** and **8** may derive from the different properties of central metal ions, that is, the well-known effect of lanthanide contraction.[20]

As shown in Figure 8a, each samarium ion is bridged by three TBDC ligands, and every TBDC ligand connects two samarium ions, forming a two-dimensional honeycomb layer framework. Six samarium ions occupy six corners of the six-sided wax cells in a honeycomb layer with diagonal distances of 21.381 Å, 20.501 Å, and 19.483 Å. It should be pointed out the 2D layers adopt an AAAA stacking arrangement along the *a* axis (Figure 8b),[23] where one water and two DMF guests reside in each hexagon (Figure S4).

It is worthy to note that there exist strong hydrogen bonding interactions between the coordinated water molecules and the carbonyl oxygen atom of uncoordinated DMF molecules with O···O distances of 2.759 Å and 2.811 Å. Each uncoordinated DMF molecules connect two layered frameworks through hydrogen bonds, as shown in Figure 9a. Thus, the adjacent alternative layers are held together along the *c* axis by hydrogen-bonding interactions, generating a three-dimensional porous structure (Figure S5). If the central samarium ions could be considered as four-connected nodes and TBDC ligands and the hydrogen bonds as the linear linkers, the stacking of these layers lead to a diamond topology (Figure 9). Two such networks interpenetrate each other to stabilize the whole structure, as shown in Figure 9c.

3.2. Gas-Adsorption Properties. On the basis of the calculation with PLATON, the solvent-accessible volume for complexes **5**, **6**, **7**, and **8** are 38.9%, 50.7%, 42.7%, and 25.8%, respectively. In order to check the permanent porosity of these porous materials, gas-adsorption tests for complexes **5**−**8** were conducted in different conditions.

Gas adsorption results of **5** are shown in Figure 10. Before gas-adsorption measurement, the sample was soaked in

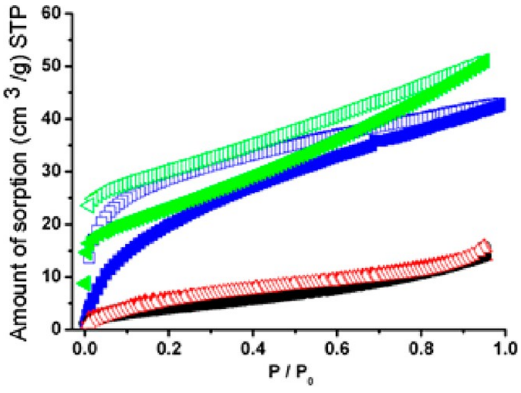

Figure 10. The sorption isotherms of complex **5** at 77 K. Black, N_2; red, Ar; green, CO_2; blue, H_2.

methanol for 24 h, and then vacuum-dried at 120 °C for 5 h. However, the N_2 and Ar (kinetic diameter: 3.64 Å for N_2 and 3.54 Å for Ar) sorption isotherm did not indicate any appreciable amount of adsorption, presumably due to the limited pore size. However, the activated **5** can adsorb a moderate amount of CO_2 (51 $cm^3\ g^{-1}$) and H_2 (56 $cm^3\ g^{-1}$, 0.49 wt %), with type-I behaviors. Derived from the CO_2 adsorption data, complex **5** has a Langmiur surface area of 141 m^2/g. Considering the kinetic diameters of 2.89 Å for H_2, 3.3 Å for CO_2, and 3.54 Å for Ar, it can be speculated that the pore opening of activated **5** should fall into the range from 3.3 to 3.54 Å, which only allows CO_2 and H_2 to enter the channels.

dx.doi.org/10.1021/cg400531j | *Cryst. Growth Des.* 2013, 13, 3154−3161

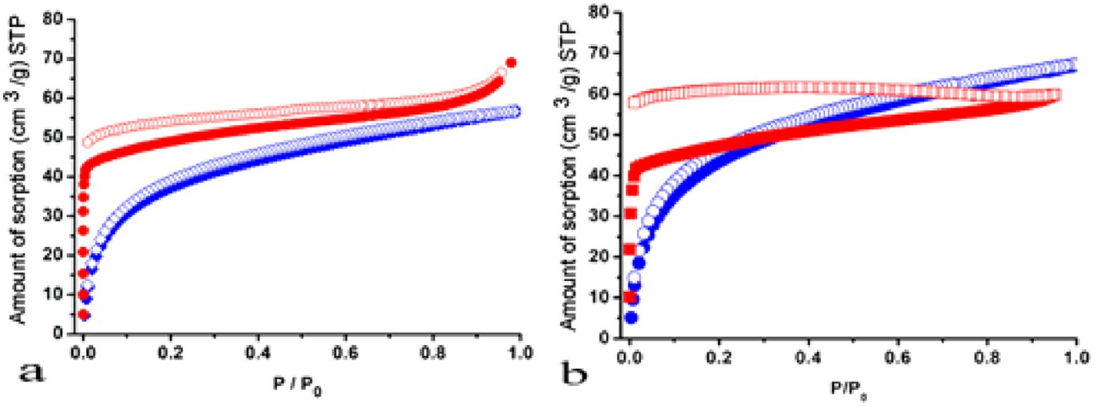

Figure 11. (a) Gas sorption isotherm of **6** at 77 K. Red, N_2; blue, H_2; (b) Gas sorption isotherm of **7** at 77 K. Red, N_2; blue, H_2.

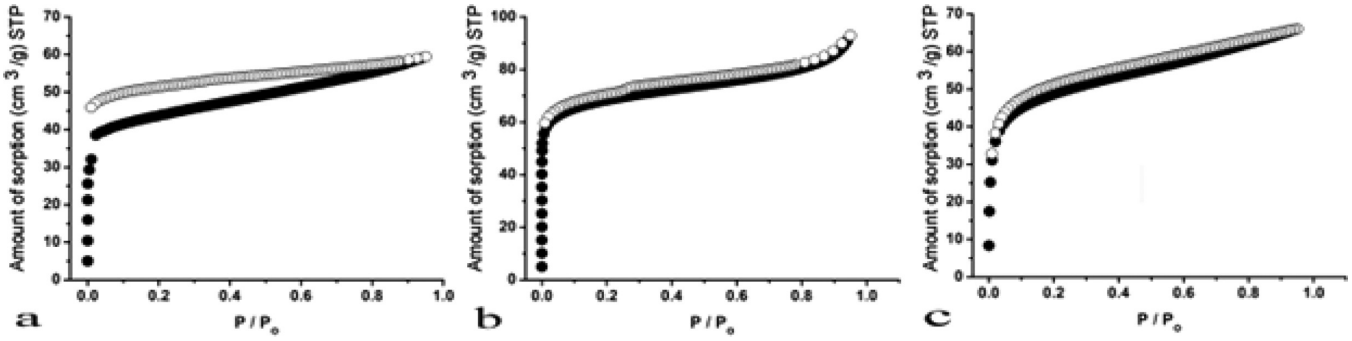

Figure 12. Gas sorption isotherms of complex **6** (a) Ar at 77 K, (b) O_2 at 77 K, and (c) CO_2 at 195 K.

The gas-adsorption behaviors of the activated **6**, which had been vacuum-dried at 120 °C after being soaked in methanol for several hours, reveal that complex **6** can retain its framework after the removal of the solvates. Complex **6** can adsorb a moderate amount of N_2 (69 $cm^3\ g^{-1}$), Ar (59.4 $cm^3\ g^{-1}$), O_2 (93 $cm^3\ g^{-1}$), and H_2 (56.6 $cm^3\ g^{-1}$, 0.5 wt %) at 77 K, and CO_2 (66 $cm^3\ g^{-1}$) at 195 K, with type-I behaviors and a Langmuir surface area of 219 m^2/g based on the N_2 adsorption data (Figures 11a and 12). The lower gas-adsorption amounts may derive from the existence of large and straight channels without any cages or polyhedra in the structure.[24]

Complex **7** was activated at 220 °C and tested for N_2 and H_2 at 77 K. Complex **7** could absorb a moderate amount of N_2 (59.8 $cm^3\ g^{-1}$), H_2 (68.0 $cm^3\ g^{-1}$, 0.6 wt %) with type-I behaviors and a Langmuir surface area of 254 m^2/g based on the N_2 adsorption data (Figure 11b). The H_2 sorption of **7** is slightly higher than that of **6**, which may be the result of the removal of solvates from the large channels. The N_2 isotherm of **7** displayed a significant hysteresis between sorption and desorption curves, compared to others. Compared to **6**, the slight decrease of N_2 sorption mount of **7** further indicates that the solvent-accessible volume has a significant influence on the gas adsorption. The N_2 sorption mount of complexes **6** and **7** are obvious more than that of **5**, presumably due to the following reason: large steric hindrance groups limit the range of the pore size and reduce the solvent-accessible volume.

Complex **8** was activated at 100 °C under a vacuum for 10 h. Dinitrogen-adsorption test showed that complex **8** could absorb a moderate amount of N_2 (187.11 $cm^3\ g^{-1}$) with type-I behavior and has a Langmuir surface area of 755.24 m^2/g derived from the N_2 adsorption data (Figure 13). The minor hysteresis in the isotherms may derive from the sliding of the layers.

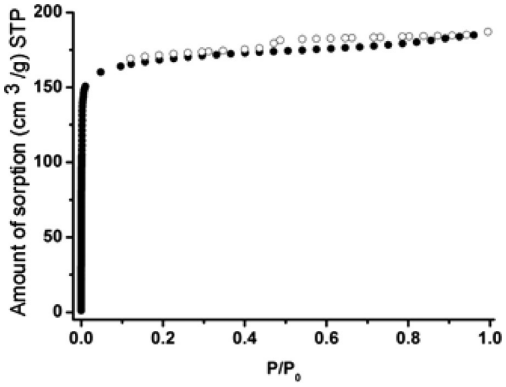

Figure 13. Nitrogen sorption isotherm of **8** at 77 K.

3.3. Catalytic Test for 6.

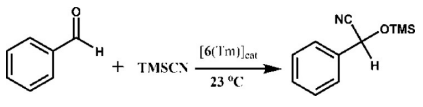

Considering that complex **6** has large channels and high thermal stability, the Lewis acid-catalyzed reaction of carbonyl compounds with cyanide was carried out to test its catalytic property. The sample of **6** was activated at 200 °C under vacuum for 5 h before the catalytic test. Complex **6** showed moderate activity in the cyanosilylation of benzaldehyde and 57.4% conversion was reached in 5 h. Recently, Zou group synthesized a series of $[Ln(btc)(H_2O)]$·guest (Nd (1), Sm (2),

dx.doi.org/10.1021/cg400531j | Cryst. Growth Des. 2013, 13, 3154−3161

Eu (3), Gd (4), Tb (5), Ho (6), Er (7), and Yb (8); H_3btc = 1,3,5-benzenetricarboxylic acid; guest: DMF or H_2O) complexes and tested their catalytic activity.[25] The results revealed that the activity of the Ln(btc) catalysts decreased with the reduction of the ionic radius of the Ln(III) ions. Thus, it is reasonable that the catalytic activity of complex **6** is compared to [Er(btc)(H_2O)] and [Yb(btc)(H_2O)] complexes due to the similar ionic radius of Er, Tm, and Yb ions. As is known, ketones are much less reactive than aldehydes. Thus, the cyanosilylation catalyzed by complex **6** (2 mol %) at room temperature for 15 h gave only 8.0% yield for acetophenone.

4. CONCLUSION

In summary, two isomorphous 3D interpenetrating lanthanide−organic frameworks were synthesized (**1** and **2**, labeled as type I). Because of the interpenetration, there are no channels in this type of structure. Through control over interpenetration or changing reaction condition, three other types of lanthanide−organic frameworks (**3**−**8**) with improved gas adsorption properties have been constructed. Results and conclusions of these investigations are summarized as follows: (1) the replacements of 1,4-benzenedicarboxylic acid with its derivative, 2,3,5,6-tetramethyl-1,4-benzenedicarboxylic acid containing hindrance groups, and coordinated solvates with chelating phen ligand in complexes **3**, **4**, and **5**, have effectively controlled the interpenetration without changing the original topology, while limiting the size of the pore and showing gas adsorption selectivity; (2) the use of rigid rod-shaped SBU in complexes **6** and **7** has significantly improved the thermal stability; (3) thermal sliding or breathing of a 2D layer may generate porous material (as found in complex **8**), which provides a new strategy on the construction of porous MOFs. It is known that the capability of gas storage for an MOF is highly determined by the channel geometry and the ligand functionality.[26] Our studies provide some effective strategies on improving gas storage capability of porous MOFs. It is believed that these results presented here may open a promising avenue to rational design and synthesis of porous lanthanide MOFs with gas storage capability or selectivity.

■ ASSOCIATED CONTENT

Supporting Information

Crystallographic data in CIF format, additional figures of gas adsorptions, powder X-ray diffractions (PXRD) patterns and the thermogravimetric analysis for complexes−**8**. This material is available free of charge via the Internet at http://pubs.acs.org.

■ AUTHOR INFORMATION

Corresponding Author

*E-mail: dfsun@upc.edu.cn, dfsun@sdu.edu.cn.

Author Contributions

§(H.H. and H.M.) These authors contributed equally.

Notes

The authors declare no competing financial interest.

■ ACKNOWLEDGMENTS

This work was supported by the NSFC (Grant Nos. 90922014, 21001115, 21271117), NCET-11-0309 and the Shandong Natural Science Fund for Distinguished Young Scholars (JQ201003), and the Fundamental Research Funds for the Central Universities (13CX05010A).

■ REFERENCES

(1) For recent reviews, see: (a) Kitagawa, S.; Kitaura, R.; Noro, S. *Angew. Chem., Int. Ed.* **2004**, *43*, 2334. (b) Ferey, G.; Mellot-Draznieks, C.; Serre, C.; Millange, F. *Acc. Chem. Res.* **2005**, *38*, 217. (c) Bradshaw, D.; Claridge, J. B.; Cussen, E. J.; Prior, T. J.; Rosseinsky, M. J. *Acc. Chem. Res.* **2005**, *38*, 273. (d) Murray, L. J.; Dinca, M.; Long, J. R. *Chem. Soc. Rev.* **2009**, *38*, 1294. (e) Lee, J. Y.; Farha, O. K.; Roberts, J.; Scheidt, K. A.; Nguyen, S. T.; Hupp, J. T. *Chem. Soc. Rev.* **2009**, *38*, 1450. (f) Aakeroy, C. B.; Champness, N. R.; Janiak, C. *CrystEngComm* **2010**, *12*, 22. (g) Phan, A.; Doonan, C. J.; Uribe-Romo, F. J.; Knobler, C. B.; O'Keeffe, M.; Yaghi, O. M. *Acc. Chem. Res.* **2010**, *43*, 58. (h) Sumida, K.; Rogow, D. L.; Mason, J. A.; McDonald, T. M.; Bloch, E. D.; Herm, Z. R.; Bae, T.-H.; Long, J. R. *Chem. Rev.* **2012**, *112*, 724−781. (i) Suh, M. P.; Park, H. J.; Prasad, T. K.; Lim, D.-W. *Chem. Rev.* **2012**, *112*, 782−835.

(2) (a) Moulton, B.; Lu, J. J.; Hajndl, R.; Hariharan, S.; Zaworotko, M. J. *Angew. Chem., Int. Ed.* **2002**, *41*, 2821. (b) An, J.; Geib, S. J.; Rosi, N. L. *J. Am. Chem. Soc.* **2009**, *131*, 8376. (c) Koh, K.; Wong-Foy, A. G.; Matzger, A. J. *J. Am. Chem. Soc.* **2009**, *131*, 4184. (d) Ma, L. Q.; Lin, W. B. *Angew. Chem., Int. Ed.* **2009**, *48*, 3637. (e) Liu, Y. L.; Eubank, J. F.; Cairns, A. J.; Eckert, J.; Kravtsov, V. Ch.; Luebke, R.; Eddaoudi, M. *Angew. Chem., Int. Ed.* **2007**, *46*, 3278. (f) Fang, Q. R.; Zhu, G. S.; Xue, M.; Sun, J. Y.; Wei, Y.; Qiu, S. L.; Xu, R. R. *Angew. Chem., Int. Ed.* **2005**, *44*, 3845. (g) Bourne, S. A.; Lu, J. J.; Mondal, A.; Moulton, B.; Zaworotko, M. J. *Angew. Chem., Int. Ed.* **2001**, *40*, 2111.

(3) (a) Farha, O. K.; Mulfort, K. L.; Thorsness, A. M.; Hupp, J. T. *J. Am. Chem. Soc.* **2008**, *130*, 8598. (b) Banerjee, M.; Das, S.; Yoon, M.; Choi, H. J.; Hyun, M. H.; Park, S. M.; Seo, G.; Kim, K. *J. Am. Chem. Soc.* **2009**, *131*, 7524. (c) Higuchi, M.; Tanaka, D.; Horike, S.; Sakamoto, H.; Nakamura, K.; Takashima, Y.; Hijikata, Y.; Yanai, N.; Kim, J.; Kato, K.; Kubota, Y.; Takata, M.; Kitagawa, S. *J. Am. Chem. Soc.* **2009**, *131*, 10336. (d) Guo, Z. G.; Cao, R.; Wang, X.; Li, H. F.; Yuan, W. B.; Wang, G. J.; Wu, H. H.; Li, J. *J. Am. Chem. Soc.* **2009**, *131*, 6894. (e) Zhang, J.; Chen, S. M.; Zingiryan, A.; Bu, X. H. *J. Am. Chem. Soc.* **2008**, *130*, 17246.

(4) (a) Zhang, J.; Wu, T.; Chen, S. M.; Feng, P. Y.; Bu, X. H. *Angew. Chem., Int. Ed.* **2009**, *121*, 3486. (b) Ma, L. Q.; Mihalcik, D. J.; Lin, W. B. *J. Am. Chem. Soc.* **2009**, *131*, 4610. (c) Zhang, Y. B.; Zhang, W. X.; Feng, F. Y.; Zhang, J. P.; Chen, X. M. *Angew. Chem., Int. Ed.* **2009**, *48*, 5287−5290. (d) Cui, H. B.; Zhou, B.; Long, L. S.; Okano, Y.; Kobayashi, H.; Kobayashi, A. *Angew. Chem., Int. Ed.* **2008**, *47*, 3376. (e) Nelson, A. P.; Farha, O. K.; Mulfort, K. L.; Hupp, J. T. *J. Am. Chem. Soc.* **2009**, *131*, 458−460. (f) He, Y. B.; Xiang, S. C.; Chen, B. L. *J. Am. Chem. Soc.* **2011**, *133*, 14570.

(5) (a) Fang, Q. R.; Zhu, G. S.; Xue, M.; Sun, J. Y.; Wei, Y.; Qiu, S. L.; Xu, R. R. *Angew. Chem., Int. Ed.* **2005**, *117*, 3913. (b) Lan, A. J.; Li, K. H.; Wu, H. H.; Olson, D. H.; Emge, T. J.; Ki, W.; Hong, M. C.; Li, J. *Angew. Chem., Int. Ed.* **2009**, *48*, 2334. (c) Ohara, K.; Marti-Rujas, J.; Haneda, T.; Kawano, M.; Hashizume, D.; Izumi, F.; Fujita, M. *J. Am. Chem. Soc.* **2009**, *131*, 3860. (d) Wang, X. L.; Qin, C.; Wu, S. X.; Shao, K. Z.; Lan, Y. Q.; Wang, S.; Zhu, D. X.; Su, Z. M.; Wang, E. B. *Angew. Chem., Int. Ed.* **2009**, *48*, 5291. (e) Nijemk, N.; Thissen, P.; Yao, Y.; Longo, R. C.; Roodenko, K.; Wu, H.; Zhao, Y.; Cho, K.; Li, J.; Langreth, D. C.; Chabal, Y. J. *J. Am. Chem. Soc.* **2011**, *133*, 12849. (f) Chapman, K. W.; Sava, D. F.; Halder, G. J.; Chupas, P. J.; Nenoff, T. M. *J. Am. Chem. Soc.* **2011**, *133*, 18583.

(6) (a) Subramanian, S.; Zaworotoko, M. J. *Angew. Chem., Int. Ed.* **1995**, *34*, 2127. (b) Abrahams, B. F.; Hoskins, B. F.; Michail, D. M.; Robson, R. *Nature* **1994**, *369*, 727.

(7) (a) Ma, S.; Yuan, D.; Wang, X.; Zhou, H.-C. *Inorg. Chem.* **2009**, *48*, 2072. (b) Dimos, A.; Tsaousis, D.; Michaelides, A.; Skoulika, S.; Golhen, S.; Ouahab, L.; Didierjean, C.; Aubry, A. *Chem. Mater.* **2002**, *12*, 2616. (c) Pan, L.; Huang, X.; Li, J.; Wu, Y.; Zheng, N. *Angew. Chem., Int. Ed.* **2000**, *39*, 527.

(8) (a) Chen, X.-Y.; Zhao, B.; Shi, W.; Xia, J.; Cheng, P.; Liao, D.-Z.; Yan, S.-P.; Jiang, Z.-H. *Chem. Mater.* **2005**, *17*, 2866. (b) Sun, D. F.; Cao, R.; Liang, Y. C.; Shi, Q.; Hong, M. C. *J. Chem. Soc., Dalton Trans.* **2002**, 1847. (c) Black, C. A.; Costa, J.; Fu, W. T.; Massera, C.; Roubeau, O.; Teat, S. J.; Aromi, G.; Gamez, P.; Reedijk, J. *Inorg. Chem.*

2009, *48*, 1062. (d) de Lill, D. T.; Cahill, C. L. *Chem. Commun.* **2006**, 4946. (e) Liang, Y. C.; Cao, R.; Su, W. P.; Hong, M. C.; Zhang, W. J. *Angew. Chem., Int. Ed.* **2000**, *112*, 3442.
(9) (a) Zhao, X. J.; Zhu, G. S.; Fang, Q. R.; Wang, Y.; Sun, F. X.; Qiu, S. L. *Cryst. Growth Des.* **2009**, *9*, 737. (b) Wu, J.-Y.; Yeh, T.-T.; Wen, Y.-S.; Twu, J.; Lu, K.-L. *Cryst. Growth Des.* **2006**, *6*, 467. (c) Huang, W.; Wu, D.; Zhou, P.; Yan, W. B.; Guo, D.; Duan, C. Y.; Meng, Q. J. *Cryst. Growth Des.* **2009**, *9*, 1361. (d) Zhou, Y. F.; Jiang, F. L.; Yuan, D. Q.; Wu, B. L.; Wang, R. H.; Lin, Z. Z.; Hong, M. C. *Angew. Chem., Int. Ed.* **2004**, *43*, 5665.
(10) (a) Luo, J.; Xu, H.; Liu, Y.; Zhao, Y.; Daemen, L. L.; Brown, C.; Timofeeva, T. V.; Ma, S.; Zhou, H. -C. *J. Am. Chem. Soc.* **2008**, *130*, 9626. (b) Ma, S. Q.; Wang, X. S.; Yuan, D. Q.; Zhou, H. −C. *Angew. Chem., Int. Ed.* **2008**, *47*, 4130. (c) Devic, T.; Serre, C.; Audebrand, N.; Marrot, J.; Férey, G. *J. Am. Chem. Soc.* **2005**, *127*, 12788. (d) Lin, Z. J.; Yang, Z.; Liu, T. F.; Huang, Y. B.; Cao, R. *Inorg. Chem.* **2012**, *51*, 1813. (e) Dai, F. N.; Sun, D.; Sun, D. F. *Cryst. Growth Des.* **2011**, *11*, 5670. (f) Yang, J.; Song, S.- Y.; Ma, J.-F.; Liu, Y.-Y.; Yu, Z.-T. *Cryst. Growth Des.* **2011**, *11*, 5469. (g) White, K. A.; Chengelis, D. A.; Gogick, K. A.; Stehman, J.; Rosi, N. L.; Petoud, S. *J. Am. Chem. Soc.* **2009**, *131*, 18069.
(11) (a) Sun, D.; Ke, Y.; Mattox, T. M.; Parkin, S.; Zhou, H.-C. *Inorg. Chem.* **2006**, *45*, 7566. (b) Zhao, D.; Yuan, D. Q.; Sun, D. F.; Zhou, H. -C. *J. Am. Chem. Soc.* **2009**, *131*, 9186.
(12) (a) He, H.; Yuan, D.; Ma, H.; Sun, D.; Zhang, G.; Zhou, H.-C. *Inorg. Chem.* **2010**, *49*, 7605. (b) Shattock, T.; Vishweshwar, P.; Wang, Z.; Zaworotko, M. J. *Cryst. Growth Des.* **2005**, *5*, 2046. (c) He, H.; Dai, F.; Xie, A.; Tong, X.; Sun, D. *CrystEngComm* **2008**, *10*, 1429. (d) He, H.; Collins, D.; Dai, F.; Zhao, X.; Zhang, G.; Ma, H.; Sun, D. *Cryst. Growth Des.* **2010**, *10*, 895.
(13) (a) Shekhah, O.; Wang, H.; Paradinas, M.; Ocal, C.; Schupbach, B.; Terfort, A.; Zacher, D.; Fischer, R. A.; Woll, C. *Nat. Mater.* **2009**, *8*, 481. (b) Ma, L. Q.; Lin, W. B. *J. Am. Chem. Soc.* **2008**, *130*, 13834. (c) Ma, S. Q.; Sun, D. F.; Ambrogio, M.; Fillinger, J. A.; Parkin, S.; Zhou, H.-C. *J. Am. Chem. Soc.* **2007**, *129*, 1858. (d) Wang, Q.; Zhang, J. Y.; Zhuang, C. F.; Tang, Y.; Su, C. Y. *Inorg. Chem.* **2009**, *48*, 287.
(14) Rosi, N. L.; Kim, J.; Eddaoudi, M.; Chen, B. L.; O'Keeffe, M.; Yaghi, O. M. *J. Am. Chem. Soc.* **2005**, *127*, 1504.
(15) (a) Zhang, J. J.; Wojtas, L.; Larsen, R. W.; Eddaoudi, M.; Zaworotko, M. J. *J. Am. Chem. Soc.* **2009**, *131*, 17040. (b) Farha, O.; Malliakas, C. D.; Kanatzidis, M. G.; Hupp, J. T. *J. Am. Chem. Soc.* **2010**, *132*, 950.
(16) (a) Park, H. J.; Suh, M. P. *Chem.—Eur. J.* **2008**, *14*, 8812. (b) Kondo, A.; Noguchi, H.; Carlucci, L.; Proserpio, D.; Ciani, G.; Kajiro, H.; Ohba, T.; Kanoh, H.; Kaneko, K. *J. Am. Chem. Soc.* **2007**, *129*, 12362.
(17) (a) Kolotuchin, S. V.; Thiessen, P. A.; Fenlon, E. E.; Wilson, S. R.; Loweth, C. J.; Zimmerman, S. C. *Chem.—Eur. J.* **1999**, *5*, 2537. (b) He, H.; Dai, F.; Sun, D. *Dalton Trans.* **2009**, 763.
(18) (a) Sheldrick, G. M. *SHELXS-97, Program for Crystal Structure Solution*; Gottingen University: Germany, 1997. (b) Sheldrick, G. M. *SHELXL-97, Program for Crystal Structure Refinement*; Gottingen University: Germany, 1997.
(19) (a) Han, Y. F.; Li, X. Y.; Li, L. Q.; Ma, C. L.; Shen, Z.; Song, Y.; You, X. Z. *Inorg. Chem.* **2010**, *49*, 10781. (b) Zhang, Z. H.; Wan, S. Y.; Okamura, T.; Sun, W. Y.; Ueyama, N. *Z. Anorg. Allg. Chem.* **2006**, *632*, 679. (c) Zhang, W. Z. *Acta Crystallogr., Sect. E: Struct. Rep. Online* **2006**, *62*, No. m1600.
(20) Pan, L.; Zheng, M.; Wu, Y.; Han, S.; Yang, R.; Huang, X.; Li, J. *Inorg. Chem.* **2001**, *40*, 828.
(21) (a) Guo, X. D.; Zhu, G. S.; Sun, F. X.; Li, Z. Y.; Zhao, X. J.; Li, X. T.; Wang, H. C.; Qiu, S. L. *Inorg. Chem.* **2006**, *45*, 2581. (b) Reineke, T. M.; Eddaoudi, M.; Keeffe, M. O.; Yaghi, O. M. *Angew. Chem., Int. Ed.* **1999**, *38*, 2590. (c) Serre, C.; Millange, F.; Marrot, J.; Ferey, G. *Chem. Mater.* **2002**, *14*, 2409.
(22) (a) Spek, A. L. *J. Appl. Crystallogr.* **2003**, *36*, 7. (b) Spek, A. L. *PLATON, A Multipurpose Crystallographic Tool*; Utrecht University: Utrecht, The Netherlands, 2006; available via http://www.cryst.chem.uu.nl/platon (for Unix) and http://www.chem.gla.ac.uk/louis/software/platon/ (for MS Windows).
(23) (a) Zaworotko, M. J. *Chem. Commun.* **2001**, 1. (b) Zhao, X.; He, H.; Dai, F.; Sun, D.; Ke, Y. *Inorg. Chem.* **2010**, *49*, 8650.
(24) (a) Rowsell, J. L. C.; Yaghi, O. M.; Chen, B. L.; Ockwig, N. W.; Millward, A. R.; Contreras, D. S. *Angew. Chem., Int. Ed.* **2005**, *44*, 4647. (b) Wang, X.-S.; Ma, S. Q.; Forster, P. M.; Yuan, D. Q.; Eckert, J.; López, J. J.; Murphy, B. J.; Parise, J. B.; Zhou, H.-C. *Angew. Chem., Int. Ed.* **2008**, *47*, 7263. (c) Wang, X.-S.; Ma, S. Q.; Rauch, K.; Simmons, J. M.; Yuan, D. Q.; Wang, X. P.; Yildirim, T.; Cole, W. C.; López, J. J.; de Meijere, A.; Zhou, H.-C. *Chem. Mater.* **2008**, *20*, 3145. (d) Nouar, F.; Eckert, J.; Eubank, J. F.; Forster, P.; Eddaoudi, M. *J. Am. Chem. Soc.* **2009**, *131*, 2864.
(25) (a) Gustafsson, M.; Bartoszewicz, A.; Martin-Matute, B.; Sun, J. L.; Grins, J.; Zhao, T.; Li, Z. Y.; Zhu, G. S.; Zou, X. D. *Chem. Mater.* **2010**, *22*, 3316. (b) Song, F.; Wang, C.; Falkowski, J. M.; Ma, L.; Lin, W. B. *J. Am. Chem. Soc.* **2010**, *132*, 15390.
(26) Chun, H.; Dybtsev, D. N.; Kim, H.; Kim, K. *Chem.—Eur. J.* **2005**, *11*, 3521.